MOISTURE PROFILE WORKSHOP NOTES

Department of Conservation and Land Management

Western Australia

W.U.R.C. Harvey

14 November 1989

Dr John Davis
Applied Physics Department
Chisholm Institute of Technology
Caulfield East
Victoria

Mr Jugo Ilic
CSIRO
Division of Forestry and Forest Products
Highett
Victoria

1. INTRODUCTION

Radiation densitometry is a technique which has been used since the early 1960's for determining the density characteristics of wood samples. In recent years, the use of x-ray and gamma-ray sources together with direct computer control has become popular in various wood research centres.

These more recent wood densitometry techniques make use of radioisotope sources and solid state radiation detectors instead of radiation sensitive film to measure the transmission of radiation through wood samples. As a result, control of a densitometry scan and the processing of data can be done much more efficiently and safely.

A direct scanning x-ray densitometer was built by the Applied Physics Department at Chisholm Institute of Technology some years ago. The instrument funded by the Australian Timber Research Institute, is at the CSIRO Division of Forestry and Forest Products. Designed for thin, 2mm thick, increment core samples, this low energy x-ray instrument is able to produce accurate density (late wood - early wood) profiles of wood samples.

In 1988, CALM commissioned a feasibility study to assess the viability of gamma-ray densitometry to measure both the density and moisture content variation and distribution in thick timber samples during drying from the green state. Results of this study have shown that it is possible to obtain accurate and absolute values of density and moisture content distribution in timber during seasoning. A new direct scanning gamma-ray densitometer has been designed subsequent to this study.

2. X-RAYS AND GAMMA-RAYS

X-rays and gamma-rays are essentially electromagnetic radiation just as are ultra-violet, visible, infra-red and microwave radiations. The relative position of these radiation phenomena in the electromagnetic spectrum is shown in Figure 1. Identification of these forms of electromagnetic radiation in the spectrum is determined by the nature of their production, their range of wavelengths or energy and the way in which they interact with matter.

It is often incorrectly assumed that x-rays and gamma-rays are somehow different; with gamma-rays being more potent than x-rays. In fact they are the same physical entity. The present day usage of the terms x and gamma is a consequence of the historical discovery of this class of electromagnetic radiation. If it is necessary to make a distinction then one turns to way in which x-rays/gamma-rays are produced. Once produced, there is no difference.

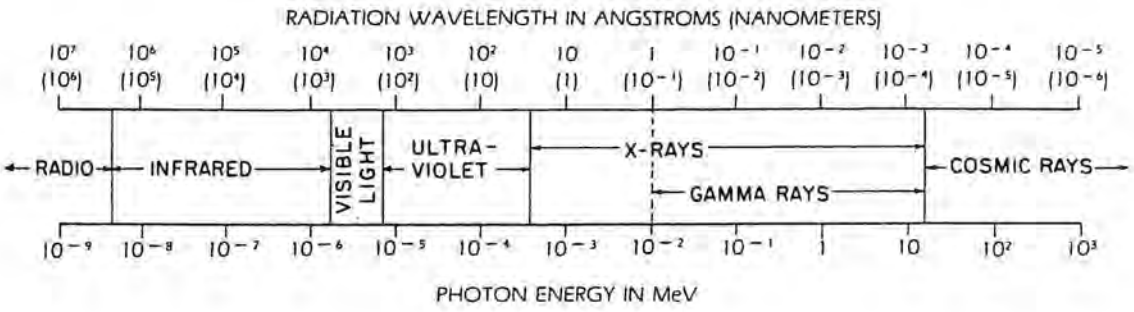

Figure 1. The electromagnetic spectrum.

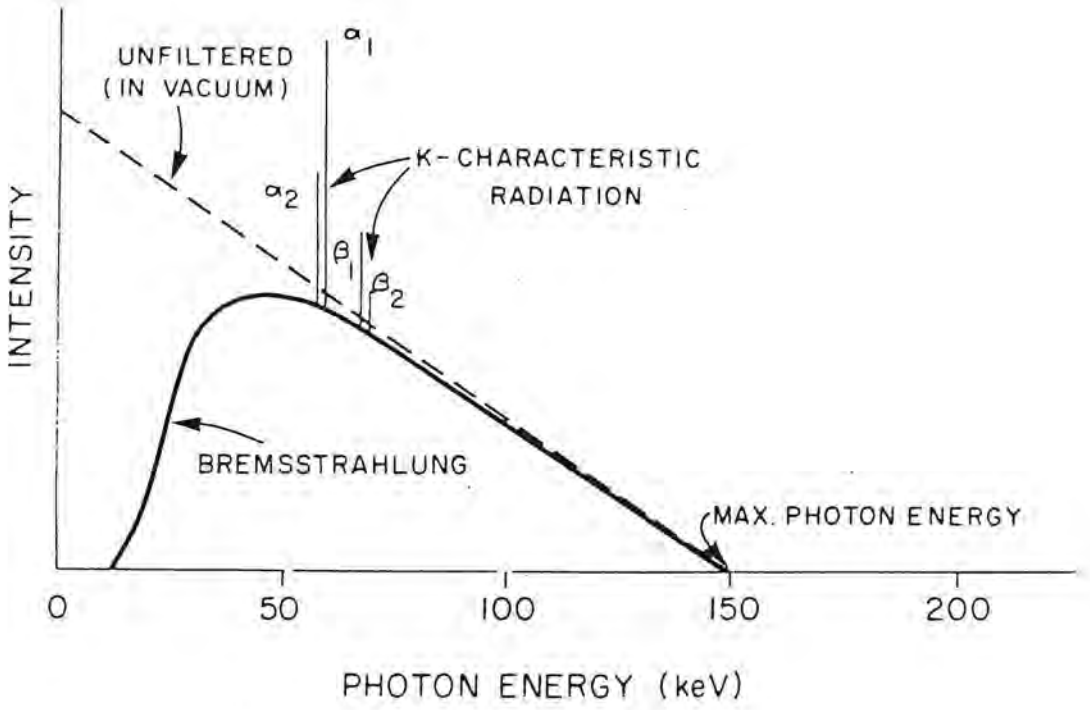

Figure 2. Typical output spectrum from an x-ray tube.

2.1 Production of x-rays and gamma-rays

In practice, x-rays are produced in an x-ray tube. This is an evacuated glass chamber in which a beam of electrons is accelerated by high voltages from 20,000 volts up to 400,000 volts on to a target material. The target material is usually a pure metal such as copper, molybdenum or tungsten. Interaction of the high energy electrons with the atomic electrons in the target gives rise to a broad energy spectrum of x-rays called bremmstrahlung (braking) radiation and a number of discrete x-ray energies characteristic of the target material as shown in Figure 2. Very high energy x-rays can also be generated in devices called linear accelerators or LINACS in which electrons are accelerated by voltages in excess of 1 million volts.

Gamma-rays are generated by radioactive isotopes. Discrete energy changes within the nucleus of a radioactive or unstable atom gives rise to the emission of corresponding discrete electromagnetic radiations or gamma-rays. Unlike the production of x-rays, radioisotopes do not produce the continuous bremmstrahlung radiation only a well defined set of characteristic gamma-ray energies.

Radioactive sources do not require electrical power and are generally considerably cheaper than x-ray generation equipment. However, x-ray sources generate a much larger flux of radiation (up to 10,000 times) than do gamma-ray sources.

2.2 Energy units

X-rays and gamma-rays are often referred to in terms of their energy. The energy unit employed is the electron volt (eV). By definition, an electron volt is the energy acquired by an electron (e) when accelerated through a voltage difference of one volt (V). In x-ray tubes, electrons give up their energy to produce x-rays. Since thousands of volts are employed in x-ray systems, x-rays will have energies of thousands of electron volts, keV, or even millions of electron volts, MeV in the case of LINACS. Gamma-rays similarly have the same energy units and may have energies ranging from a few tens of keV and upwards. Hence it is possible for x-rays to have higher energies than gamma-rays.

2.3 Radiation safety

Both x-rays and gamma-rays present a human tissue health hazard. Consequently some form of biological shielding must be employed to protect operators from radiation exposure. The type and bulk of material used for shielding will depend upon the energy and intensity of the radiation source. Also the radiation flux emanating from a shielded radiation source must be suitably collimated or shaped so that the radiation flux is directed in a usually well defined manner. Design of appropriate shielding and collimators is usually straight forward task.

Installation and use of a radiation source requires the approval of state government health authorities before licensing can be granted. Users of equipment employing such sources must also be accredited by the same authorities. Appropriate radiation health monitoring is also a requirement for user personnel.

Good equipment design and the common sense of user personnel will ensure the safe operating condition of radiation equipment.

3. INTERACTION OF X-RAYS AND GAMMA-RAYS WITH MATTER

In wood densitometry work the energy of the radiation employed is less than 100keV. The gamma-ray densitometer developed for CALM uses a radioactive isotope of americium-241 (Am-241) which emits gamma-rays having an energy of 59.5keV.

To understand the interaction of x-ray or gamma-ray radiation with matter it is convenient to consider the radiation as a stream of particle-like packages of energy called photons. Thus each of the photons emitted from Am-241 has an energy of 59.5keV.

When a narrow collimated beam of gamma-ray photons (a pencil beam) is directed into a material, the photons may be either absorbed by atoms or scattered out of the beam by the electrons around the atoms. The process of absorption and scattering which reduces the number of photons in the beam is referred to as attenuation.

3.1 Attenuation processes in materials

There are three photon attenuation processes of significance in densitometry work, photoelectric absorption, Rayleigh scattering and Compton scattering.

(a) Photoelectric absorption

In this interaction (Figure 3) a photon is totally absorbed by an atom and ejects an electron from the atom.

(b) Rayleigh scattering

In this scattering process the incident photons have their directions changed after interacting with the atomic electrons. The energy of the photon is not changed in this interaction (Figure 3).

(c) Compton scattering

This process involves the interaction of an incident gamma-ray photon and an electron in the material. At higher gamma-ray energies, the Compton interaction is the dominant attenuating process in wood.

In Compton scattering the incoming gamma-ray is deflected through an angle θ with respect to its incident direction. The photon transfers some of its incident energy to the recoil electron as shown in Figure 3. At low incident energies, the gamma-ray photons are scattered in all directions with roughly equal probability.

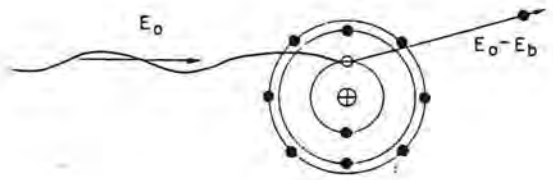

(a)

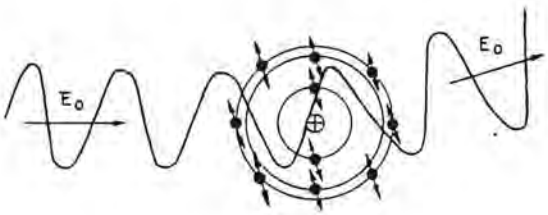

(b)

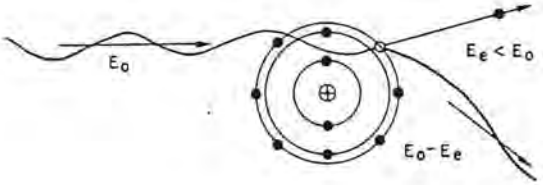

(c)

Figure 3. The three gamma-ray interaction phenomena in materials relevant to densitometry work. In the photoelectric effect (a) the incoming gamma-ray photon is totally absorbed and ejects an electron from the atom. Ragleigh scattering (b) arises when the gamma radiation is scattered out of its incident direction by the electrons of an atom without energy loss. A Compton scattering (c) event occurs when gamma-ray photons are scattered by an electron losing some of its energy to the recoil electron.

3.2 Attenuation coefficients

When a narrow beam of gamma-ray photons is directed into a material the above interaction will remove some photons from the beam. The number of photons in the beam which survive the passage through the material without interaction is then a measure of the amount of material in the path of the beam.

Figure 4(a) shows a narrow beam of photons of incident intensity I_o (the number of photons incident per second) entering a slab of material of thickness t. The probability that photons will pass through the slab without being absorbed or scattered (ie., attenuated) is

$$\text{Probability of survival} = e^{-\mu t}$$

where μ is called the total linear attenuation coefficient of the material in the beam path and is a measure of the probability of photon interaction per unit length of material - the larger is t, the higher is the probability of interaction. We may express μ as

$$\mu = \mu_{\text{Photoelectric}} + \mu_{\text{Rayleigh}} + \mu_{\text{Compton}}$$

showing that it is the sum of all three attenuating processes.

The value of μ depends upon a number of factors:

(i) The energy of the gamma-ray radiation.

(ii) The density of the material.

(iii) The atomic number of the atomic species which make up the material.

When the gamma-ray energy is fixed then the latter two factors affect μ. For equilibrated wood specimens in which the atomic composition is uniform throughout the wood, μ is directly proportional to the wood density.

The intensity I of photons transmitted through the slab of material is given by

$$\begin{bmatrix}\text{Number of photons}\\ \text{transmitted}\end{bmatrix} = \begin{bmatrix}\text{Number of incident}\\ \text{photons}\end{bmatrix} \times \begin{bmatrix}\text{Probability}\\ \text{of}\\ \text{survival}\end{bmatrix}$$

or

$$I = I_o e^{-\mu t} \qquad (1)$$

Figure 4(b) shows how I varies with t for a given material of linear attenuation coefficient μ. Equation (1) is the basis of the densitometry technique.

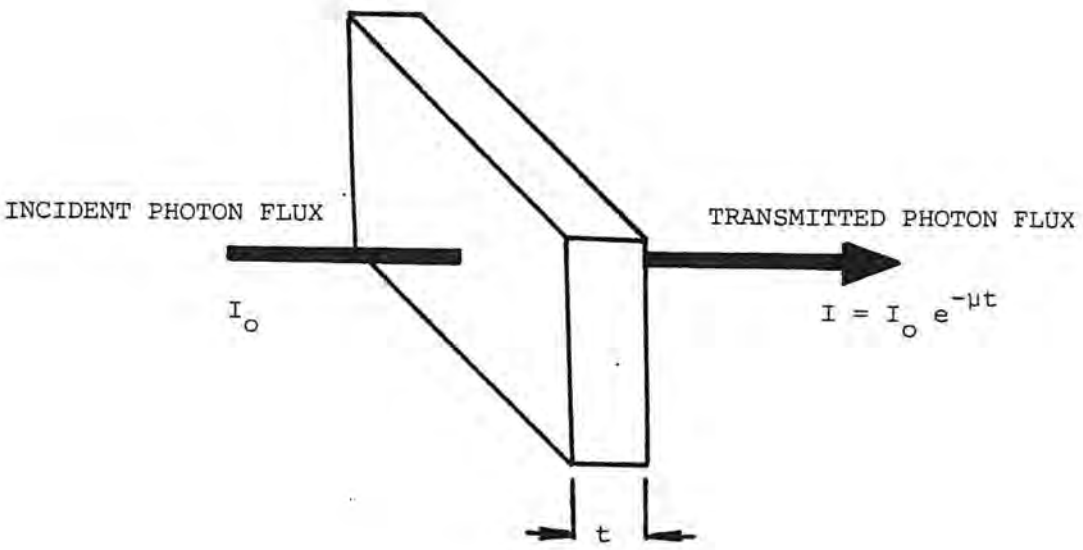

(a)

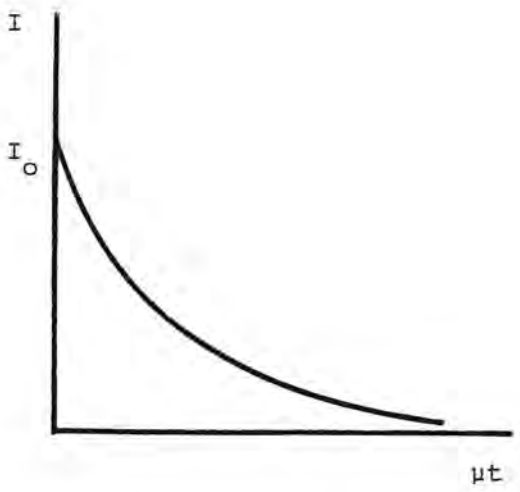

(b)

Figure 4: (a) Transmission of a narrow beam of gamma-ray photons through a slab of material of thickness t.

(b) Variation of the transmitted photons as a function of the product μt.

In densitometry work it is often convenient to use the quantity, mass attenuation coefficient μ_m in m^2/kg. This quantity represents the probability of photon attenuation per unit mass of material in the path of the beam. The quantities μ and μ_m are related by

$$\mu = \mu_m \rho = \left(\frac{\mu}{\rho}\right)\rho \qquad (2)$$

where ρ is the bulk density in kg/m^3 of the attenuating material. Substituting equation (2) into equation (1) gives

$$I = I_o e^{-\mu_m \rho t} \qquad (3)$$

Transforming equation (3) yields

$$\mu_m \rho t = \ln[I_o/I] \qquad (4)$$

where $\ln(I_o/I)$ is the natural logarithm of the ratio of the incident or unattenuated photon intensity to the transmitted intensity. Hence for a material of known thickness and mass attenuation coefficient, the average bulk density of material in the path of the beam is given by

$$\rho = \frac{1}{\mu_m t} \ln[I_o/I] \qquad (5)$$

If the gamma-ray beam has a cross-sectional area A, the volume of material through which the beam passes is At. A measurement of ρ is thus a measure of the mass of material in the volume At defined by the beam.

If as shown in Figure 5, the material is moved stepwise through the beam, each step increment being the width w of the beam, then the bulk density (or mass of material) can be determined at each step position. A plot of bulk density versus position along the scan direction would then represent the density profile of the material cross-section in the beam direction. This plot also represents the net mass profile of the same cross-section.

In the discussion above, the material was assumed to consist of one atomic species only. Wood on the other hand contains a mixture carbon, oxygen, hydrogen, nitrogen and various trace elements. The average mass attenuation coefficient for a mixture of N elements is determined from

$$\bar{\mu}_m = \sum_{i=1}^{N} f_i \, \mu_{m_i} \qquad (6)$$

where $\bar{\mu}_m$ is the average mass attenuation coefficient of the mixture, f_i is the weight fraction of the ith element with mass attenuation coefficient μ_{m_i}. Thus if the composition by weight of the wood

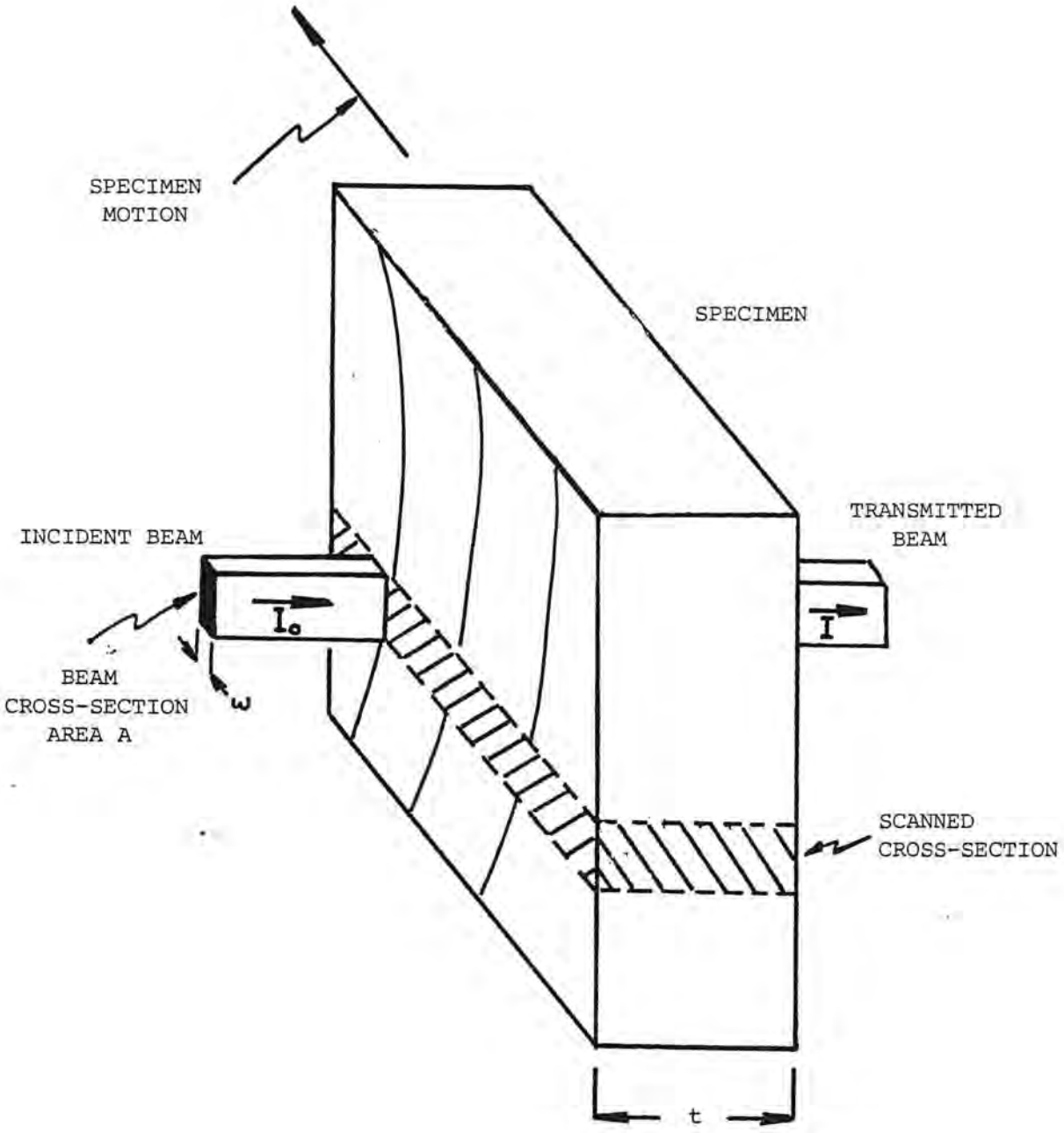

Figure 5: Experimental arrangement for gamma-ray densitometry. The beam geometry is defined by collimators before and after the specimen. For a beam of cross-section area A, a volume At is sampled at each step of the specimen motion. The shaded region represents the section of the specimen examined in a densitometry scan.

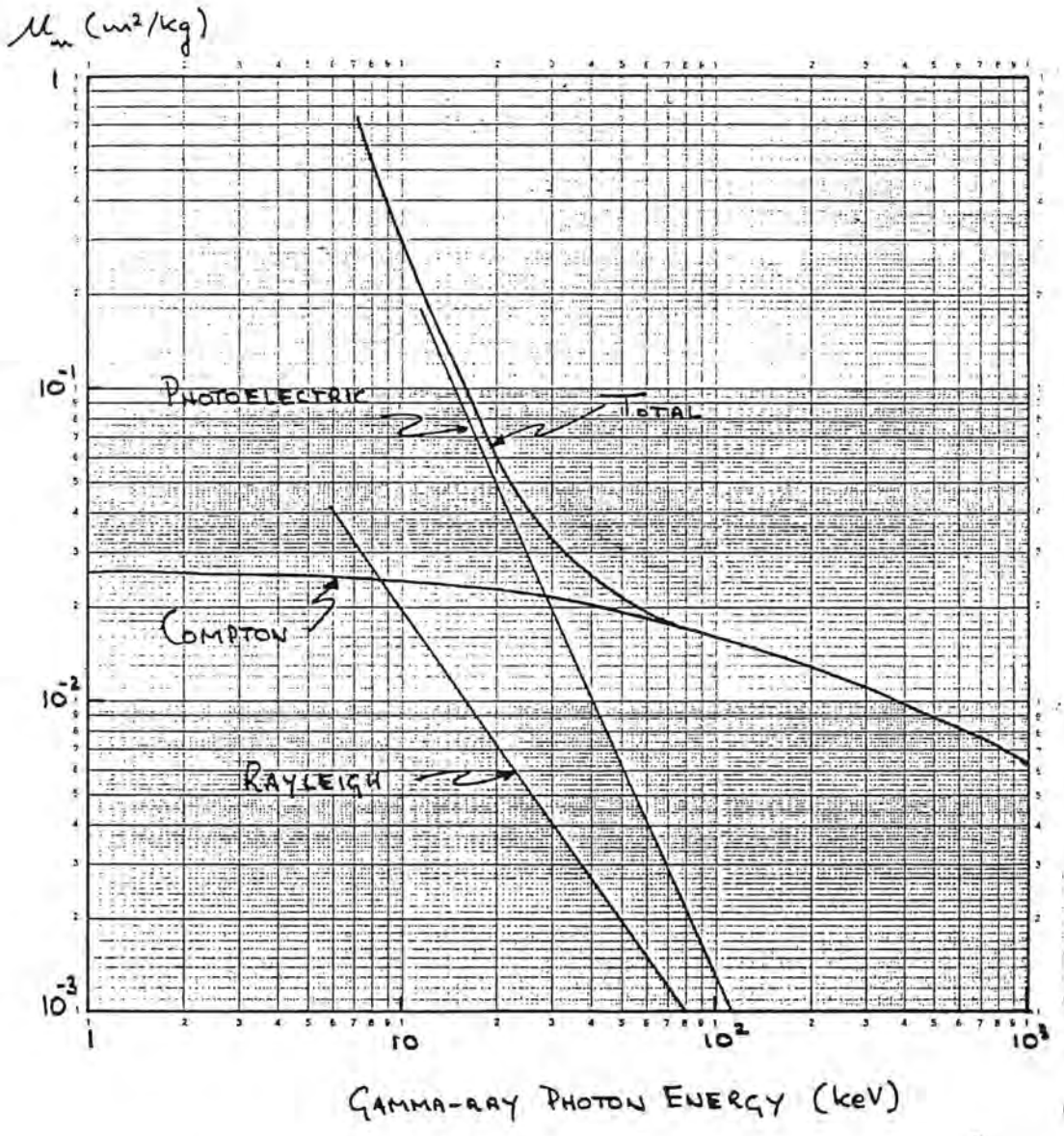

Figure 6. The variation of the mass attenuation coefficient μ_m with photon energy for dry wood. Compton scattering is the dominant attenuation effect at higher gamma-ray energies.

matrix is known, $\bar{\mu}_m$ can be calculated using the available theoretical values of μ_m for each element.

A plot of the average mass attenuation coefficient of oven dry wood versus gamma-ray energy is shown in Figure 6. Note that as photon energy increases, the energy dependence of the attenuation process shifts from domination by the photoelectric process to that of Compton scattering.

3.3 A cautionary note

Equation (1) can be written in the form

$$\mu t = \ln(I_o/I)$$

and

$$\mu = \frac{1}{t} \ln(I_o/I) \qquad (7)$$

In a measurement we know t and measure I_o and I so that the value of μ is obtained without ambiguity.

On the other hand from equation (4) we have

$$\mu_m \rho = \frac{1}{t} \ln(I_o/I) \qquad (8)$$

and unless μ_m is known, then the value of ρ cannot be determined and only the product $\mu_m \rho$ (ie., μ) is obtained. This is not a problem for equilibrated wood specimens in which moisture is uniformly distributed but presents difficulties in unequilibrated material containing a variation of moisture content and hence μ_m.

4. THE DIRECT SCANNING GAMMA-RAY DENSITOMETER

In this section the operation of the direct scanning gamma-ray densitometer is described. Although the instrument employs a radioactive isotope as the radiation source, an x-ray tube could be substituted for this source if required.

4.1 Description of the densitometer

Figure 7 shows the schematic arrangement of the densitometer. The instrument consists of a number of modules including:

* Radiation source and shielding
* Radiation beam collimators
* Radiation detector
* Photon counting electronics
* Specimen translation bench including a stepper motor

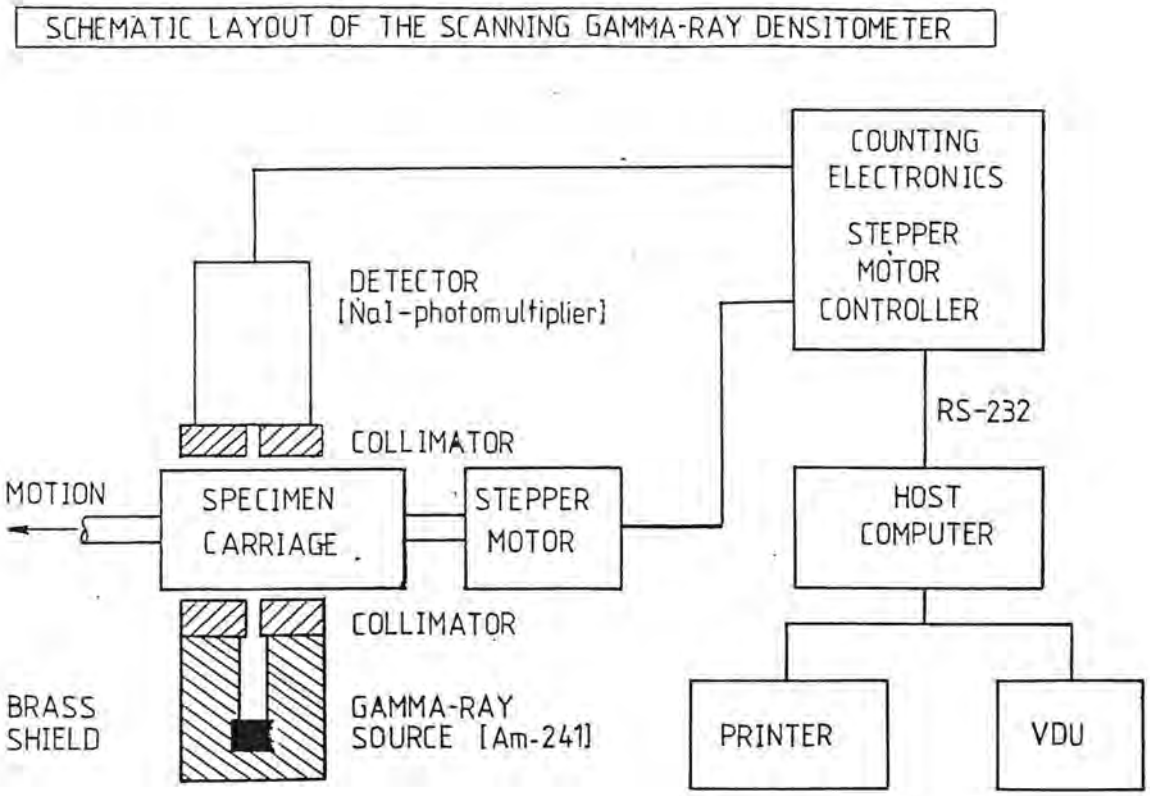

Figure 7. The schematic layout of the CALM gamma-ray scanning densitometer.

* Stepper motor power supply and controller

* Microcomputer and peripherals

* Data acquisition and processing software.

4.1.1 Radiation source and shielding

The radiation source is a 5mm diameter 200 milliCurie pellet of americium-241 in a sealed stainless steel cylinder enclosed in a radiation shield source holder made of brass. Brass is a satisfactory shielding material for this source. The smallest shielding thickness of the source holder is 23.5mm. This reduces the photon transmission by a factor of about 10^{-11} so that the radiation level at the surface of the shielding is negligible. A blank brass cap containing a lead disc is placed over the radiation beam exit hole of the shield when the instrument is not in use. The shielding design has been approved by the Radiation Health Board of W.A.

4.1.2 Beam collimators

These are also made of brass. The collimators are designed to fit over the end of the source shield and the front of the radiation detector. Rectangular slits in the collimators define the shape of the beam and constrain the radiation to a straight line between source and detector. The beam is 50mm above the specimen carriage.

Three pairs of collimators having slit heights of 4mm and widths of 0.25mm, 0.5mm and 1mm can be used depending on the resolution required in a scan. An horizontal micrometer adjustment on the source shield enables the source and detector collimators to be accurately aligned. The collimators have been designed so that the beam remains aligned when collimators are interchanged.

4.1.3 Radiation detector

This is a commercially available NaI scintillator-photomultiplier detector. Photons arriving at the detector are converted to voltage pulses; one pulse for each photon. These pulses are transmitted to the counting electronics and thence to the microcomputer for storage and processing.

4.1.4 Counting electronics

To minimise costs, a custom made electronics system was designed to count photons arriving at the detector. The system selects only those voltage pulses corresponding to the photons from the source and rejects any other pulses. A high voltage supply for the photomultiplier is also incorporated in the system.

Counting of photons can be achieved in two ways; preset time mode or preset count mode. In the preset time mode, the counter accumulates photon pulses for a predetermined time period. Since the number of counts obtained will vary depending on the density of the wood specimen, the statistical uncertainty in the measured density will vary from point to point in a scan. When operating in the preset count mode, pulses are accumulated until the preset value is reached.

The time taken to reach this preset limit is then related to the density of the specimen. In this mode all data obtained has the same statistical uncertainty. That is to say, one can predetermine the precision of a measurement.

All of the counting parameters can be set up from the microcomputer keyboard prior to a scanning measurement.

4.1.5 Specimen translation bench

This consists of a lead screw driven by a stepper motor under instruction from the microcomputer. The specimen is mounted on a carriage attached to the lead screw and can be moved stepwise through the radiation beam. A scan is completed when the specimen has been translated through the beam from end to end. Specimens up to 300mm in length and 160mm thick (in the beam direction) can be accommodated. The specimen is held in position on the carriage table by magnets.

4.1.6 Stepper motor power supply and controller

This unit has been designed to be operated under instruction from the microcomputer. All stepper motor functions and hence translation bench motion can be set from the computer keyboard.

4.1.7 Microcomputer and peripherals

The microcomputer (IBM compatible) is connected via a single RS232 link to the stepper motor and counting systems. Densitometer data acquisition and control is handled by the computer. Output of raw and processed data is made to a VDU screen and can be transferred to a printer.

4.1.8 Data acquisition and processing software

The software consists of a suite of programmes written in GWBASIC consisting of

* Scan measurement (data acquisition and system control)
* Density profile and histogram analysis
* Density difference and histogram analysis
* Moisture content profile and histogram analysis
* Data file output. All data files generated can be sent to either the VDU screen or printer
* Water attenuation coefficient measurement
* Collimator alignment

A description of the data analysis procedure is given in section 5.

5. PROCESSING OF DENSITOMETRY DATA

A description of the processing of the raw gamma-ray transmission data to obtain density profile and moisture profile information from a wood specimen is presented. It is assumed that the wood specimen is in the form of a slab of thickness t.

As pointed out earlier, data may be gathered in either the preset time or preset count mode. Calculations based on either mode will be presented.

The initial part of this section will deal with specimens having an equilibrated moisture content (EMC). Treatment of unequilibrated moisture content specimens in which moisture is non-uniformly distributed will follow.

5.1 Preset time and preset count modes

In the preset time mode, photon counting continues for a predetermined time T_p. The counts accumulated in this time will be denoted as C.

For the preset count mode, the time to accumulate a predetermined number of counts C_p will be denoted as T. Note that the value of T is the sum of a number, n, of small timing increments ΔT. These timing increments are selected from the computer keyboard. Thus $T = n\Delta T$ represents a whole number of discrete time intervals elasped upon reaching C_p.

5.2 Measurement procedure

Prior to beginning a scan the following information must be obtained:

* Thickness of the specimen through which the gamma-ray beam will be transmitted, t.

* Bulk density of the specimen, ρ_{bulk}.

The scan measurement programme requests the following information:

* Specimen details.

* Collimator slit width. This will determine the linear stepping increment of the specimen carriage and the spatial resolution in the scan profile.

* Preset time or count parameters.

This information is then written into a specimen description file.

Before beginning the scan, the specimen carriage is driven to a start position and remains there until five measurements of the unattenuated air count C_o (preset time mode) or T_o (preset count mode) is obtained. The average value of C_o or T_o is then used as a

reference to determine when the specimen has completed its motion through the gamma-ray beam. Once the air count procedure is completed the carriage is moved stepwise through the beam collecting data C_i (preset time mode) or T_i (preset count mode) at each step position. Data at each step is transferred to the computer and stored in a raw data file. The density profile is also computed and displayed on the VDU screen during the measurement.

At the end of the scan the system resets the carriage to the start position. This can also be done manually by the operator if required.

5.3 Processing data from equilibrated specimens

To avoid problems associated with the gamma-ray beam overlapping the ends of the specimen, the first three and last three data values of the raw specimen transmission data are discarded. Density profile values are then computed using equation (5) ie.,

$$\rho_i = \frac{1}{\bar{\mu}_m t} \ln(C_o/C_i) \quad \text{(preset time mode)} \qquad (9)$$

or

$$\rho_i = \frac{1}{\bar{\mu}_m t} \ln(T_i/T_o) \quad \text{(preset count mode)} \qquad (10)$$

where ρ_i is the average density in the path of the beam at the ith step in the scan.

The value of $\bar{\mu}_m$ is determined from

$$\bar{\mu}_m = \left[\frac{1}{Nt\rho_{bulk}}\right] \sum_{i=1}^{N} \ln(C_o/C_i) \qquad (11)$$

or

$$\bar{\mu}_m = \left[\frac{1}{Nt\rho_{bulk}}\right] \sum_{i=1}^{N} \ln(T_i/T_o) \qquad (12)$$

where N is the number of edited raw specimen data values. This assumes that the mass attenuation coefficient is a universal constant for the specimen ie., the elemental composition is uniform throughout the equilibrated specimen.

Alternatively, if the elemental composition is known at EMC, then $\bar{\mu}_m$ can be calculated from tables of theoretical values corresponding to the energy of the gamma-ray photons.

Density values including the average density are written to a file and are displayed on the VDU screen (Figure 8). If required, a histogram or probability distribution of the density values in the profile can be determined. The histogram is presented on the VDU

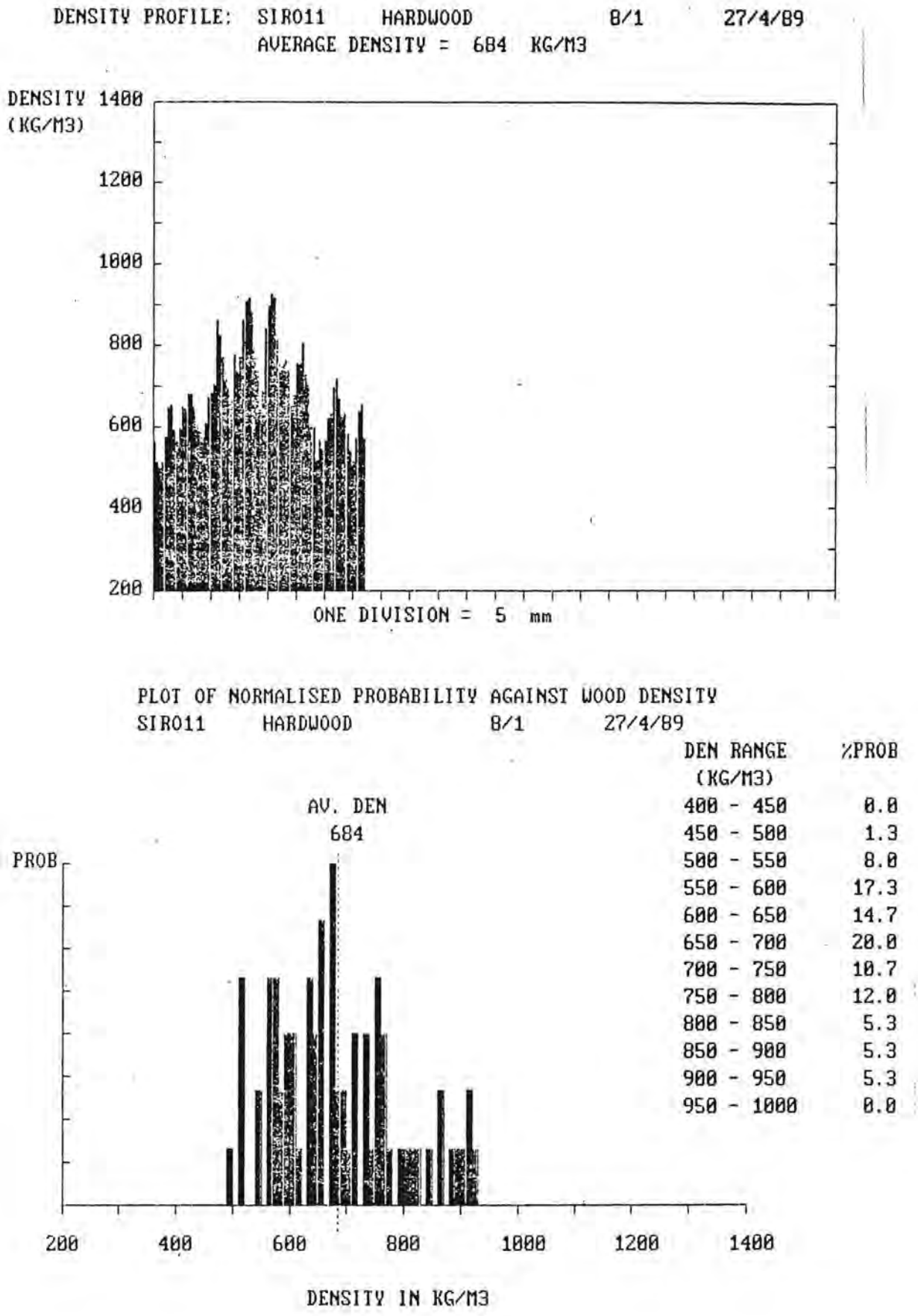

Figure 8. A typical density profile and histogram analysis of a scan of specimen removed from a sawn board.

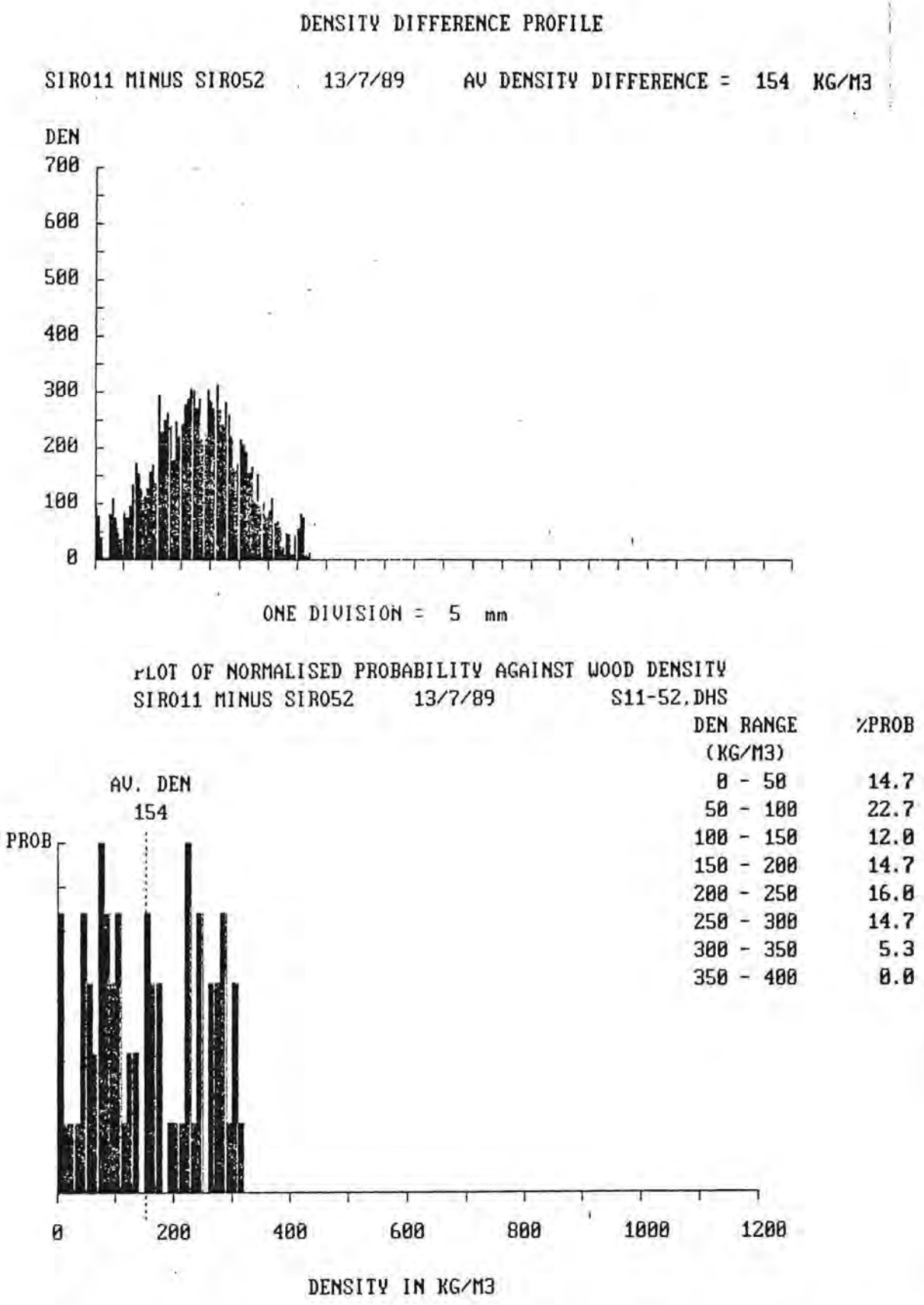

Figure 9. The density difference profile between the wet specimen of Figure 8 and its oven dry density profile. This profile also represents the water mass distribution in the scanned section of the board. An histogram analysis of the profile is also shown.

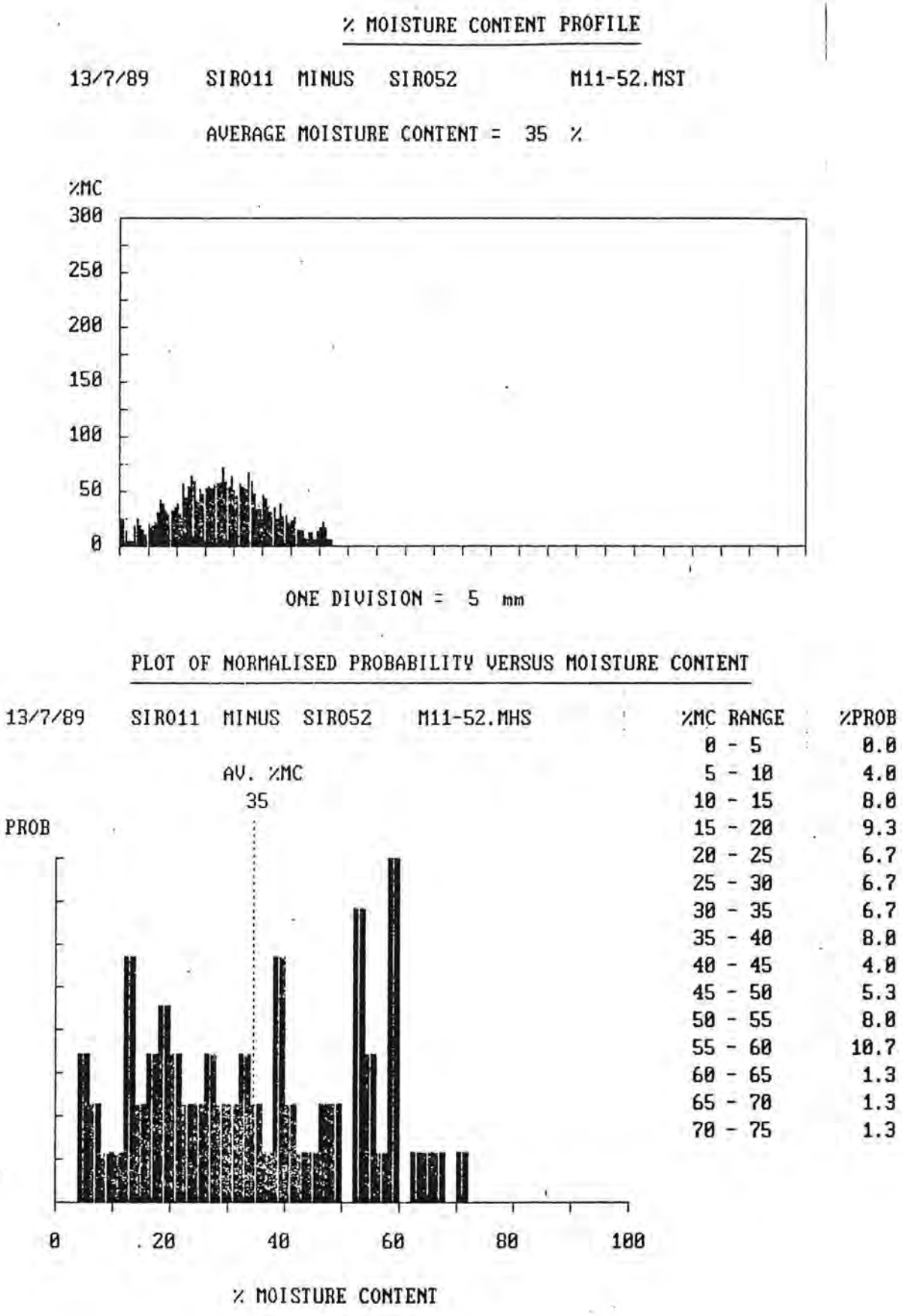

Figure 10. The moisture content profile and corresponding histogram analysis of the specimen of Figure 8.

screen (Figure 8) enabling the operator to analyse the distribution over a desired density range of data. Once the analysis is completed the data is written in a file.

Before the density difference and moisture content profiles can be obtained, the specimen must be oven dried. Prior to scanning the oven dried specimen, the information described in section 5.2 must be obtained. If the scan has been performed with the gamma-ray beam directed along the grain of the specimen then the thickness t will not change but the other dimensions will be smaller. Care must be taken to scan the oven dried specimen along the same scan line used in the initial measurement. To obtain the density difference and moisture content profiles it is necessary to correct the oven dried data for dimensional change along the scan motion direction. Once corrected the oven dried profile can be subtracted from the EMC profile in one-to-one registration. An approximate procedure for performing this operation has been developed (Section 6). Further development is needed in this area but results to data seem to indicate that the correction technique is reasonably satisfactory.

The density difference profile is determined from

$$\Delta\rho_i = \rho_{w_i} - \rho_{d_i} \qquad (13)$$

where the subscripts w and d represent the wet (EMC) density and oven dried density respectively at the ith step in the profile. Computed values including the average density difference is written to a file and displayed on the VDU screen. An histogram analysis of the density difference data is then performed (Figure 9).

Note that since the same volume of wood is sampled at each step, the density difference profile is also directly related to the moisture mass profile in the scanned section of the specimen.

Moisture content (MC) is usually defined as

$$MC = \left[\frac{\left[\begin{matrix}\text{mass of wet} \\ \text{specimen}\end{matrix}\right] - \left[\begin{matrix}\text{mass of oven} \\ \text{dried specimen}\end{matrix}\right]}{\left[\begin{matrix}\text{mass of oven} \\ \text{dried specimen}\end{matrix}\right]} \right] \times 100\% \qquad (14)$$

Thus from bulk information, the bulk MC of the specimen is obtained. The bulk moisture content for the scanned section can also be obtained from the density data as

$$MC = \left[\frac{\bar{\rho}_w \times (N_w t_w) - \bar{\rho}_d \times (N_d t_d)}{\bar{\rho}_d \times (N_d t_d)} \right] \times 100\% \qquad (15)$$

where $\bar{\rho}_w$, N_w, t_w are the average scan density, number of (edited) density values and thickness of the wet specimen data, respectively, and $\bar{\rho}_d$, N_d, t_d are the corresponding values for the oven dried state. Because of shrinkage, N_d will be less than N_w but $t_w \approx t_d$ (thickness along the grain).

The moisture content profile values of the wet specimen at each step is given by

$$MC_i = \left[\frac{\rho_{w_i} \times (N_w t_w) - \rho_{d_i} \times (N_d t_d)}{\rho_{d_i} \times (N_d t_d)} \right] \times 100\% \qquad (16)$$

Moisture profile and moisture profile histogram analysis data is written to an appropriate file and displayed on the VDU screen (Figure 10).

Note that because of the way in which MC is defined, the bulk MC of the scanned specimen section (equation (15)) cannot be calculated from the profile values of equation (16) ie.,

$$M_{bs} \neq \frac{1}{N_w} \sum_{i=1}^{N} MC_i \qquad (17)$$

5.4 Processing data from unequilibrated specimens

This section deals with the computation of density and MC profiles from specimens during drying.

In unequilibrated specimens the mass attenuation coefficient is not a constant because of the non-uniform distribution of water. Hence at each step in a scan only the quantity μ or $\mu_m \rho$ can be obtained with certainty. That is, the product of mass attenuation coefficient and density cannot be separated into two separate components. So in principle neither the density nor the moisture content can be determined unambiguously.

Fortunately, there is a way around this problem which leads to a good estimate of density and MC. The average mass attenuation coefficient of a mixture of elements was quoted as (equation (6))

$$\bar{\mu}_m = \sum_{i=1}^{N} f_i \, \mu_{m_i} \qquad (18)$$

A calculation of $\bar{\mu}_m$ for moisture contents ranging from oven dry to 200% at a gamma-ray energy of 59.5keV is shown in Table 1. In this calculation, the oven dry matrix of wood was assumed to contain (in weight %) 50% carbon, 44% oxygen and 6% hydrogen - nitrogen and trace element contributions were neglected.

Over the MC range 0 to 200%, $\bar{\mu}_m$ varies from 0.0191m^2/kg to 0.020m^2/kg, a variation of 5%. If we choose $\bar{\mu}_m$ for wood specimens to be midway in this range or 0.0195m^2/kg, then a calculation of density from either equation (9) or (10) will involve an uncertainty of about 3% or $\pm$ 25kgm^{-3} in a density value of 1000kg/m^3. The corresponding uncertainty in moisture content is about 8%. For computed MC values of 200% and 10% this represents uncertainties of $\pm$ 16MC% and $\pm$ 1MC%, respectively. In most applications this degree of uncertainty is

Table 1. Values of the average mass attenuation coefficient $\overline{\mu}_m$ of wood at a gamma-ray energy of 59.5keV over a range of moisture contents from oven dry to 200%.

MC%	Weight % of constituents			$\overline{\mu}_m$ (m^2/kg)
	Carbon	Oxygen	Hydrogen	
0	50.0	44.0	6.0	0.0190
50	33.0	58.9	7.7	0.0195
100	25.0	66.4	8.6	0.0980
200	16.7	73.9	9.3	0.0200

acceptable given that other contributions to uncertainty (specimen thickness, statistical fluctuations in photon counts etc.,) are small.

A further complicating factor arises from the non-uniform shrinkage of the specimen during drying. Determination of density difference and MC profiles involves the subtraction of one set of data from another at different MC states. In this work we subtract the oven dry specimen data from that of the wet specimen. Correction of the oven dry data for shrinkage requires that the oven dry data file contain as many values as the wet data file and that the two files be in one-to-one correspondence prior to subtraction. If local shrinkage is not large and provided collapse effects are not a severe problem, the oven dry profile data can be corrected using a simple linear interpolation scheme. This is the approach adopted at present and it seems to have been successful.

More work needs to be done to improve the shrinkage correction procedure. The present technique does not correlate the information in the wet specimen profile with the oven dry data. A more correct approach must take this into account. The ultimate correction procedure must consider localised MC gradients and dimensional changes which means that the assumption of a simple linear scheme is not strictly valid. This will be more critical when scans are done with narrow collimation or higher spatial resolution where earlywood to latewood transitions are well defined. In coarse resolution scans of 1mm steps, the problem is not so severe.

6. METHOD OF CORRECTING DATA FILES FOR SHRINKAGE

Because of shrinkage, the specimen when oven dried will have different dimensions. The longitudinal dimension along the grain (photon beam direction) will not measurably alter but the radial and tangential change appreciably, more in the tangential than the radial. Hence the scan length in the wet specimen will be longer than the oven dry scan length.

To determine the density difference (or water mass content) and hence the moisture content, the oven dry data file must be subtracted point for point from the corresponding wet data file. This will require that the oven dry file (the shorter file) be transformed or stretched so that it is the same length (have the same number of data values) as the wet file.

The present strategy for doing this is outlined as follows.

1. Let the number of data values or increments in the wet file be N_w and let N_d be the number in the oven dry file with N_w greater than N_d.

2. Denote by Δ_w, the width of a scan step increment in the wet scan file. This will of course be the same for the measured oven dry scan file.

3. We stretch the oven dry file increments, each of the same width, so that the stretched increment width is denoted by Δ_s. Thus for the wet and stretched files to be of equal length

$$N_d\Delta_s = N_w\Delta_w$$

The dry data in each increment Δ_s of the stretched dry file is the same as that in the corresponding increments Δ_w of the unstretched file. To transform the stretched data file into a file of the same increment width Δ_w and length (N_w values) as the wet file it is necessary to assign new values to these increments prior to the subtraction process. The scheme is graphically shown below.

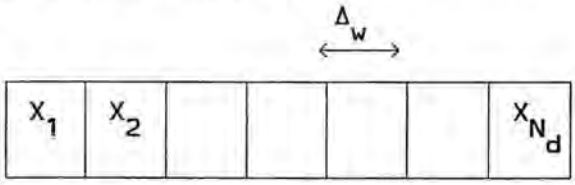

Raw oven dry file

$X_1, X_2, \ldots, X_{N_d}$ are the raw data values.

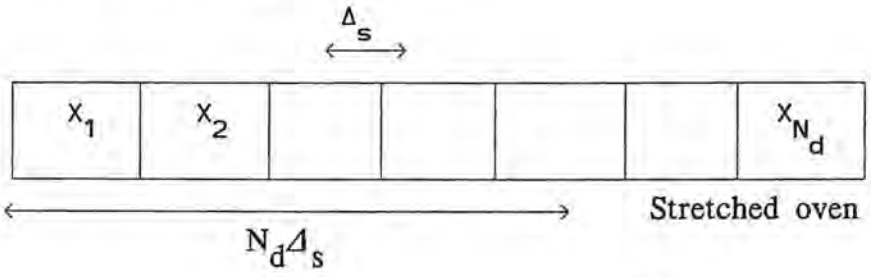

Stretched oven dry file

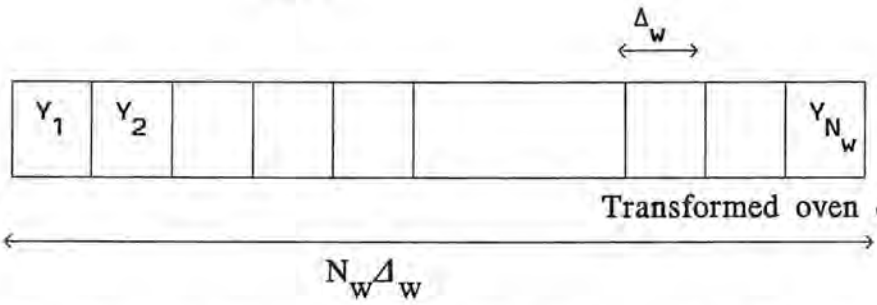

Transformed oven dry file

$Y_1, Y_2, \ldots, Y_{N_w}$ are the transformed oven dry file values.

4. Determine the set of transformed oven dry file values Y_i (with $1 \leq i \leq N_w$) from the raw values X_ℓ (with $1 \leq \ell \leq N_d$). Let D_i measure the distance from the beginning of the Y file to the right-hand end of the ith increment.

$$\therefore \quad D_i = i\Delta_w = i\Delta_s N_d/N_w$$

Let ℓ be an index which counts the increments in the stretched X file, ie.,

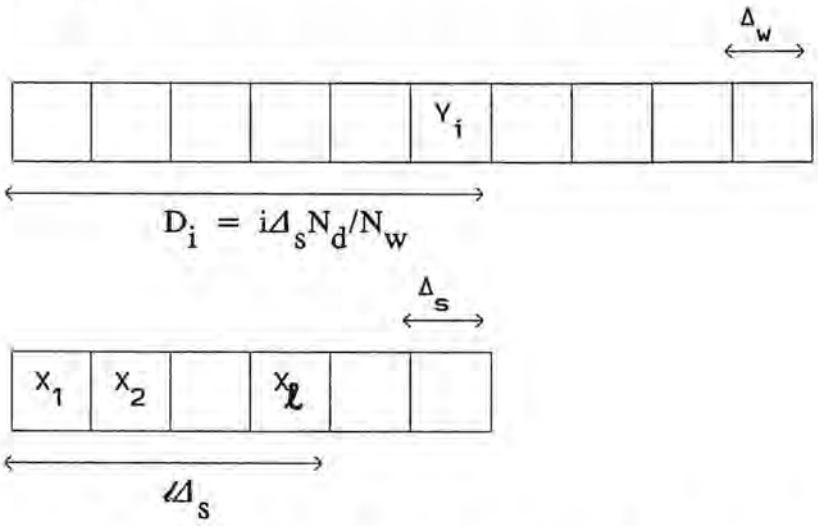

We need to know where the ith increment in the Y file is located with respect to the X file and to determine whether the ith increment in the Y file either totally overlaps a single X increment or overlaps two X increments. That is for a given i we determine the corresponding ℓ.

If we begin by letting $\ell = 1$, then

$$\Delta_{i,\ell} = D_i - \ell\Delta_s$$

$$= i\Delta_s \frac{N_d}{N_w} - \ell\Delta_s$$

If $\Delta_{i,\ell} > 0$ (positive) then increment ℓ by one so that the new value of ℓ is $\ell+1$ and recheck the difference

$$\Delta_{i,\ell} = D_i - \ell\Delta_s$$

Continue to do this until $\Delta_{i,\ell} \leq 0$.

When this occurs we know that the right-hand end of the ith Y increment is located either at or within the right-hand increment of the ℓth increment in the X file, ie., Y_i overlaps at least the X_ℓ increment value.

We now need to know where the left-hand end of the ith increment is located. To do this subtract an amount Δ_w from the current value of D_i.

$$\Delta_{i,\ell-1} = D_i - \Delta_w = i\Delta_s \frac{N_d}{N_w} - \Delta_s \frac{N_d}{N_w}$$

If $\Delta_{i,\ell-1} \geq 0$, then the left-hand end of the ith increment is located within the ℓth increment of the X file. We then put

$$Y_i = X_\ell$$

If $X_{i,\ell-1} < 0$, then the left-hand end of the ith increment in the Y file is located within the $(\ell-1)$th increment of the X file.

These two cases are shown graphically below.

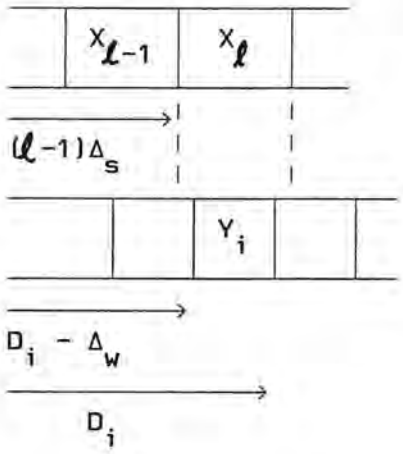

Case for $\Delta_{i,\ell-1} \geq 0$

$Y_i = X_\ell$

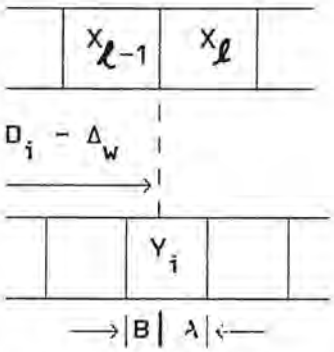

Case for $\Delta_{i,\ell-1} < 0$

In the latter case to find Y_i we need to know the lengths A and B so that the contributions to Y_i from X_ℓ and $X_{\ell-1}$ can be determined.

Now

$$A = D_i - (\ell-1)\Delta_s = i\Delta_s \frac{N_d}{N_w} - (\ell-1)\Delta_s$$

$$B = (\ell-1)\Delta_s - (i-1)\Delta_w$$

The fractional weights are

$$f_A = A/\Delta_w = A/(\Delta_s \frac{N_d}{N_w})$$

$$= i - (\ell-1) \frac{N_d}{N_w}$$

$$f_B = B/\Delta_w$$

$$= (\ell-1) \frac{N_d}{N_w} - (i-1)$$

So that

$$Y_i = X_{\ell-1} f_A + X_\ell f_B$$

As a check on the transformation process we should find that the average density in the unstretched X density file is the same as that in the stretched and transformed Y density file, ie.,

$$\frac{1}{N_d} \sum_{\ell=1}^{N_d} X_\ell = \frac{1}{N_w} \sum_{i=1}^{N_w} Y_i$$

An extension to this approach might take into account the differential nature of shrinkage. Rather than stretch all increments in the oven dry density file by the same count so that they are all width Δ_s, we could by some decision process have Δ_s values different at various points. If this were the case then at the outset we would require that

$$\sum_{j=1}^{N_d} \Delta_{s_j} = N_w \Delta_w$$

To locate the position of the ith increment of the Y density file with respect to the ℓth increment in the X density file we would check

$$\Delta_{i,\ell} = D_i - \sum_{j=1}^{\ell} \Delta_{s_j}$$

with

$$D_i = \frac{i}{N_w} \sum_{j=1}^{\ell} \Delta_{s_j}$$

and

$$\Delta_{i,\ell-1} = D_i - \Delta_w$$

so that

$$A = D_i - \sum_{j=1}^{\ell-1} \Delta_{s_j}$$

$$B = \sum_{j=1}^{\ell-1} \Delta_{s_j} - (i-1)\Delta_w$$

$$f_A = A/\Delta_w$$

$$f_B = B/\Delta_w$$

7. OPTIMISATION OF SCAN PARAMETERS

In densitometry measurements it is useful to choose conditions which enable the optimum density and moisture content sensitivities to be realised. Two parameters namely the gamma-ray photon energy (the value of the mass which determines attenuation coefficient mass attenuation coefficient) and specimen thickness are intimately involved in this optimisation process. A number of examples will be described where equilibrated specimens are used.

Within a given density profile let the density difference between two points in the specimen be ρ and $\rho+\Delta\rho$. The difference in gamma-ray transmission at these two points can be shown to be

$$\Delta P = e^{-\bar{\mu}_m \rho t} \left[1 - e^{-\bar{\mu}_m \rho t \alpha}\right] \qquad (19)$$

where $\bar{\mu}_m$ = average mass attenuation coefficient

t = specimen thickness

$\alpha = \Delta\rho/\rho$ is the density resolution

In the case of a fixed photon energy (which is the case for the CALM densitometer), $\bar{\mu}_m$ is fixed and there will be an optimum thickness which maximises ΔP. The optimum thickness in this case is

$$t_o = \frac{\ln(1+\alpha)}{\bar{\mu}_m \rho \alpha} \qquad (20)$$

For an equilibrated specimen it is then possible to obtain the optimum specimen thickness which would either:

(i) maximise the contrast between the lowest early wood density (ρ) and the highest late wood density ($\rho+\Delta\rho$). Here $\alpha = \Delta\rho/\rho$ might be of the order of 2 or more.

(ii) enable a specified density difference to be resolved. Of course the smaller α is the better must be the counting statistics (lower uncertainty).

For example, using 60keV photons with $\bar{\mu}_m = 0.019 m^2/kg$, $\rho = 500 kg/m^3$ and $\alpha = 2$, the optimum thickness is about 60mm.

When measuring in the preset time mode it is straight forward to show that if the product of $\bar{\mu}_m$ and the bulk density of a specimen ρ_b is minimised, this leads to the optimisation condition

$$\bar{\mu}_m \rho_b t \simeq 2.2 \qquad (21)$$

assuming t is accurately known. In the preset count mode there is no such optimum condition as equation. Instead the variance in $\bar{\mu}_m \rho_b t$ decreases with increasing $\bar{\mu}_m$ (or decreasing photon energy) which would be impractical since very few photons would be transmitted through the specimen.

As a rule-of-thumb it is useful when choosing the optimum thickness to adopt the condition of equation (21). The optimum condition is not very sensitive around the value 2.2 and values of $\bar{\mu}_m \rho_n t$ between 1 and 3 are often acceptable.

When measuring the moisture content profile of a specimen by subtracting the oven dry profile from the corresponding EMC profile a similar expression to equation (20) for optimum thickness is

$$t_o = \frac{\ln\left[1 + \left[\frac{\mu_m^w}{\mu_m^{wc}}\right] \frac{MC}{100}\right]}{\mu_m^w \rho_{wc} \frac{MC}{100}} \qquad (22)$$

where μ_m^w = mass attenuation coefficient of water

μ_m^{wc} = mass attenuation coefficient of dry wood

MC = % moisture content

ρ_{wc} = bulk density of dry wood

For example for MC = 75% and $\rho_{wc} = 600 kg/m^3$, $t_o \simeq 60mm$.

In unequilibrated specimens, the choice of optimum conditions is not as clear cut as is the case for equilibrated specimens. However, the above results used judiciously for unequilibrated specimens when drying from the green state should provide satisfactory results.

8. USEFUL REFERENCES

A selection of a number of publications related to x-ray and gamma-ray densitometry is given below. The publications listed have been chosen to complement the workshop notes. Although the papers address some aspects of instrumentation, densitometry theory, densitometer applications and interpretation there has not been produced to date a comprehensive publication on the practice of direct scanning wood densitometry.

* Cown, D.J. and Parker, M.L., "Comparison of annual ring density profiles in hardwoods and softwoods by x-ray densitometry", Canadian J. of Forest Research, Vol. 8, No. 4, pp442-449 (1978).

* Spolek, C.A., "A model of simultaneous convective, diffusive and capillary heat and mass transport in drying wood", Ph.D. thesis, Washington State University, pp101-119 (1981).

* Olson, J.R. and Arganbright, D.G., "Prediction of mass attenuation coefficients of wood", Wood Science, Vol. 14, No. 2, pp86-90 (1981).

* Cown, D.J. and Clement, B.C., "A wood densitometer using direct scanning with x-rays", Wood Science Technology, Vol. 17, pp91-99 (1983).

* Laufenberg, T.L., "Using gamma radiation to measure density gradients in reconstituted wood products", Forest Products Journal, Vol. 36, No. 2, pp59-62 (1986).

* Winistorfer, P.M., Davis, W.C. and Moschler, W.W., "A direct scanning densitometer to measure density profiles in wood composite products", Forest Products Journal, Vol. 36, No. 11/12, pp82-86 (1986).

* Liu, C.J., Olson, J.R., Tian, Y. and Shen, Q., "Theoretical wood densitometry: I. Mass attenuation equations and wood density models", Wood and Fiber Science, Vol. 20, No. 1, pp22-34 (1988).

* Olson, J.R., Liu, C.T., Tian, Y. and Shen Q., "Theoretical wood densitometry: II. Optimal x-ray energy for wood density measurement", Wood and Fiber Science, Vol. 20, No. 2, pp187-196 (1988).

* Moschler, W.W. and Dougal, E.F., "Calibration procedure for a direct scanning densitometer using gamma radiation", Wood and Fiber Science, Vol. 20, No. 3, pp297-303 (1988).

* Suendermann, B., "Development of a small scale x-ray computerised tomography system", M.App.Sc. Thesis, Chisholm Institute of Technology (1988).

* Veigele, W.M.J., "Atomic data tables", Vol. 5, pp51-11 (1973).